Journal of Geochemical Exploration 133 (2013) 42–49

Contents lists available at ScienceDirect

Journal of Geochemical Exploration

journal homepage: www.elsevier.com/locate/jgeoexp

Generation of Ce anomalies in SW Sardinian Mn ores

G. Mongelli [a,*], P. Mameli [b], G. Oggiano [b], R. Sinisi [b]

[a] Dipartimento di Chimica, Università degli Studi della Basilicata, Macchia Romana Campus, 85100 Potenza, Italy
[b] Dipartimento di Scienze della Natura e del Territorio, Università degli Studi di Sassari, 07100 Sassari, Italy

ARTICLE INFO

Article history:
Received 29 February 2012
Accepted 3 October 2012
Available online 9 October 2012

Keywords:
Ce anomalies
Cerianite
Sardinian Mn ores

ABSTRACT

Sedimentary (pedogenic) and hydrothermal Mn ores are hosted by a volcanic succession in south-western Sardinia. The sedimentary Mn ores are characterized by chondrite-normalized Ce anomalies (Ce/Ce*) of 1.08–3.40, whereas the hydrothermal Mn ores have Ce anomalies of 0.35–3.15.

The presence of both negative and positive Ce anomalies in the hydrothermal Mn ores is related to the remobilization of rare earth elements (REEs) within the hydrothermal system, which occurred via the dissolution and redistribution of REE-bearing accessory minerals by mineralizing fluids. The REEs were removed from wall-rocks and redeposited within the Mn ores as apatite, monazite, and cerianite, which have textures characteristic of growth into a Mn-oxide matrix during mineralization. In addition, the redistribution of cerium led to a progressive increase in the magnitude of the Ce anomaly from E to W, suggesting that mineralizing fluids moved along an E–W-striking fault close to the Mn ore.

In the sedimentary Mn ores, the spatial variability of Ce/Ce* values probably relates to changes in the deposition environment, from organic-rich to organic-poor. Positive Ce anomalies with Ce/Ce* values of 1.08–1.75 are associated with samples from thick sedimentary layers within a paleosoil or samples from veins related to paleosoils, and potentially formed in a environment where organic speciation of the REEs acted to limit cerianite precipitation. Conversely, spheroidal concretions of Mn-oxides within pumice and ash layers have larger positive Ce anomalies (Ce/Ce*>2.5) and likely formed in an organic-free environment matter, with REE speciation in circulating fluids dominated by inorganic species.

Finally, given the large range in Ce/Ce* ratios of Mn ores, we stress the need to carefully consider sampling methodologies, to ensure the accurate interpretation and determination of ore deposit models, the identification of mechanisms involved in Ce distribution, and the relationships between Ce and Mn phases.

1. Introduction

Under geological conditions, the low ionization potential of Ce(III) means that cerium often behaves differently from rare earth elements (REEs) adjacent in the periodic table (La and Pr). The Ce anomaly, Ce/Ce*, is derived from interpolation between the chondrite-normalized values of the neighboring trivalent REEs (i.e., La and Pr) to determine a value of Ce*, and it enables the identification of differing geological processes and conditions (e.g., Bau, 1999; Braun et al., 1990; Chetty and Gutzmer, 2011; Class and le Roex, 2008; Davranche et al., 2005; De Baar et al., 1983; Dia et al., 2000; Kerrich and Said, 2011; Laveuf and Cornu, 2009; Leybourne and Johannesson, 2008; Mongelli, 1997; Rankin and Childs, 1976; Seto and Akagi, 2008).

The Ce accumulation in the solid matrix may occur either as a result of cerianite (CeO_2) precipitation depending on the in situ Eh–pH conditions (Braun et al., 1990, 1998) or oxidative scavenging of Ce(IV) on the surface of Mn- and Fe-oxyhydroxides (Bau, 1999; De Carlo et al., 1998; Ohta and Kawabe, 2001). Oxidative scavenging requires sorption of REE onto Mn- and Fe-oxyhydroxides, followed by Ce oxidation induced by surface catalysis and the preferential desorption of trivalent REEs, and is often biologically mediated (Moffett, 1990, 1994; Ohnuki et al., 2008; Tanaka et al., 2010).

Mn-oxyhydroxides have a higher REE sorption capacity than Fe-oxyhydroxides at the pH conditions typically found in soils (Laveuf and Cornu, 2009, and references therein), indicating that Mn-oxyhydroxides play a significant role in promoting Ce oxidation, especially given that the Ce(III) to Ce(IV) transformation is often coupled with the reduction of Mn(IV) to Mn(III) or Mn(II) (Ohta and Kawabe, 2001). Consequently, positive Ce anomalies are often associated with Mn concretions that form during pedogenesis (e.g., Feng, 2010; Laveuf et al., 2012).

Previous studies have examined the behavior of REEs in hydrothermal systems and related ores (e.g., Bau, 1991; Chang-Bock et al., 2002; Fulignati et al., 1999; Lottermoser, 1992; Parsapoor et al., 2009; Smith et al., 2000; Terakado and Fujitani, 1998), and Gieré (1996) suggested that fluid/wall-rock interaction could cause a change in redox conditions that would lead to the oxidation of trivalent cerium and the precipitation of primary cerianite. Unfortunately, few data are available for terrestrial Mn ores; what data are available

* Corresponding author.
E-mail address: giovanni.mongelli@unibas.it (G. Mongelli).

0375-6742/$ – see front matter © 2012 Elsevier B.V. All rights reserved.
http://dx.doi.org/10.1016/j.gexplo.2012.10.002

relate to the mobility and redistribution of REEs and related accessory minerals, including cerianite, during hydrothermal alteration (Chetty and Gutzmer, 2011).

Sedimentary (pedogenic) and hydrothermal Mn ores occur in a volcanic succession in south-western Sardinia (Sinisi et al., 2012). The sedimentary Mn-ores are characterized by positive cerium anomalies (calculated on the basis of abundances normalized to chondritic values, hereafter Ce/Ce*) of 1.08–3.40, whereas the hydrothermal Mn-ores have Ce/Ce* ratios of 0.35–3.15.

This study provides the first set of REE data for both sedimentary and hydrothermal Mn ores of south-western Sardinia, and determines the processes that controlled Ce behavior and the development of the wide range in Ce/Ce* ratios during ore formation.

2. Geological setting

Sardinia is a microcontinent that was detached from the southern edge of the stable European continent during the early Miocene. The rollback of the Ligure–Piemontese oceanic slab, previously subducted below the southern European margin (Downes et al., 2001), triggered the detachment of Sardinia. Widespread subduction-related arc volcanism occurred between the Eocene–Oligocene and the Serravallian (Beccaluva et al., 1987; Lustrino et al. 2009), with the climax of the volcanic activity coincident with the onset of extension at around 18–17 Ma. This geodynamic setting induced anomalous heat flow below the western part of the Sardinian microcontinent, thus promoting hydrothermal activity (Sinisi et al., 2012) and the formation of hydrothermal ores, as reported from other back-arc settings (de Boorder et al., 1998).

The volcanic succession of western Sardinia consists of andesite domes and flows capped by variably welded rhyolite–rhyodacite pyroclastic flows and later lava flows and domes (Coulon et al., 1978). In south-western Sardinia a “Lower sequence”, consisting of andesitic rocks overlain by rhyodacitic pyroclastic flows, is capped by an “Upper sequence” of alkaline–peralkaline rhyolitic volcanic rocks, emplaced mostly as lava flows and rare pyroclastics (Morra et al., 1994). This sequence is well exposed on San Pietro and San Antioco islands, and in the Sulcis District (Assorgia et al., 1990; Fig. 1).

The magmatic products of the Upper Sequence were subaerially emplaced during the Langhian (Middle Miocene), over about 1 Ma, with magmatism initiating by 15.8 Ma at the latest (Pioli and Rosi, 2005).

The hydrothermal Mn deposits sampled during this study occur as veins in comenditic lavas and as veins and massive accumulations in welded rhyolitic ignimbrites on San Pietro Island. The sedimentary Mn deposits occur at Punta Crobettana in the Sulcis District of the mainland, adjacent to San Pietro Island. The sedimentary deposits are located between two different pyroclastic flows, and occur as thin layers within paleosoils and as Mn concretions within the underlying pyroclastic flows.

3. Occurrence of Mn ores

The distribution of Mn ores within the Langhian ignimbritic sequence is shown in Fig. 2. As stated above, epivolcanic activity on San Pietro Island led to the formation of two types of hydrothermal Mn ore: 1) in the La Piramide area, Mn concentrations occur within a welded ignimbrite as individual centimeter-wide veins and as aggregates which pseudomorph eutaxitic structures, and opal-CT and quartz are the main gangue minerals; 2) at Cala Fico, Mn ores are hosted by comenditic lavas and occur as massive-textured vein swarms that are oriented parallel to the main faults in the area. Mn-rich bands oriented parallel to rheomorphism-related anisotropic features are also common in this area. Both types of mineralization are developed close to an E–W-striking fault that juxtaposes the lower part of the comenditic lava flow sequence with the underlying ignimbrite unit (Upper Ignimbrite of Pioli and Rosi, 2005), both of

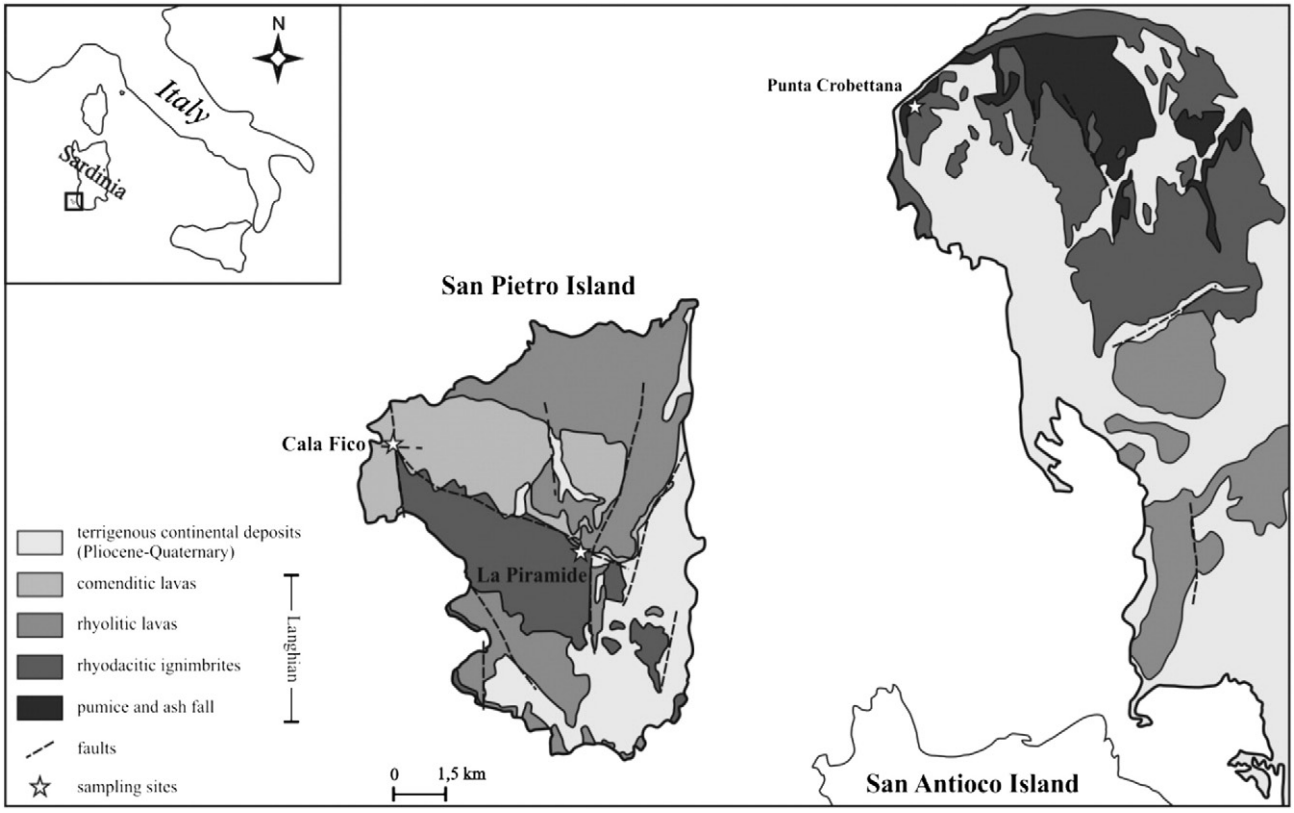

Fig. 1. Geologic sketch map of the S. Pietro Island and of the Sulcis District.

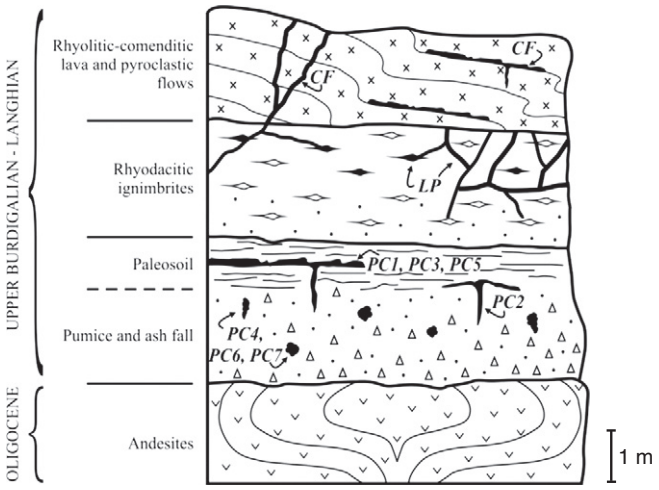

Fig. 2. The distribution of Mn ores within the ignimbritic sequence. LP: La Piramide; CF: Cala Fico; PC: Punta Crobettana.

which are Langhian in age. The ignimbrite is a high-grade, strongly welded ignimbrite with a marked foliation, fiammae sets, and a crystal-rich matrix containing abundant centimeter-size plagioclase and amphibole crystals.

The sedimentary ores at Punta Crobettana consist of centimeter-scale Mn beds and concretions at the contact between the uppermost Upper Ignimbrite and the lower, poorly welded, pedogenized tuff, corresponding to the "pumice and ash fall" deposit of Pioli and Rosi (2005). Manganese occurs as centimeter-thick beds within a 1-meter-thick, rubrified, clay-rich paleosoil. Manganese veins often extend from this clay-rich horizon into the underlying tuff, which consists of millimeter-size plagioclase, sanidine, and pyroxene crystals, with pumice lapilli and subordinate xenoclasts. Spheroidal concretions of Mn-oxides also occur around pumice and ash.

4. Sampling and analytical methods

Fifteen samples of hydrothermal Mn ore (7 from La Piramide (LP) and 8 from Cala Fico (CF)) and 7 samples of sedimentary Mn ore from Punta Crobettana (PC) were analyzed to determine their paragenesis and chemical features, including major element and REE concentrations. Only unaltered samples were collected, and care was taken to prevent contamination of the samples during collection, transport, and subsequent storage.

Whole-rock samples were dried and then reduced to fine powder in a Retsch planetary mill equipped with two agate jars and agate milling balls at the laboratories of Dipartimento di Scienze della Natura e del Territorio, University of Sassari (Italy). The mineralogy of individual samples was identified by the analysis of randomly oriented whole-rock powders using a Siemens D5000 diffractometer (Cu–Kα radiation, 40 kV, and 30 mA); data were obtained at 2°–70° 2θ with a step size of 0.02°. The petrography of samples was determined by optical transmission microscopy (OM) using a Leitz binocular microscope, and by scanning electron microscopy (ESEM) using a XL30 Philips LaB6 SEM equipped with an energy dispersive X-ray spectrometer (SEM–EDS) at the "Centro Interdipartimentale Grandi Attrezzature Scientifiche" (CIGAS) Laboratories of the University of Basilicata, Italy.

Major element and REE abundances were determined by inductively coupled plasma–mass spectrometry (ICP–MS) and instrumental neutron activation analysis (INAA), respectively, at Activation Laboratories, Ancaster, Canada. Analytical uncertainties were less than ±5%, except for elements at a concentration of 10 ppm or lower, for which uncertainties were ±5%–10%. Total loss on ignition (LOI) was determined gravimetrically after heating overnight at 950 °C.

Quantitative electron microprobe analyses of Mn phases were acquired using a scanning electron microscope TESCAN Vega 3 LMU instrument equipped with a TEAM EDS system X-ray dispersive analyzer with Apollo X SDD installed at the "Dipartimento per lo Studio del Territorio e delle sue Risorse" (DIPTERIS), University of Genoa, Italy. Operating conditions were 15 kV accelerating voltage and 2.20 nA beam current.

5. Results

5.1. Mineralogy

Mn-oxides are ubiquitous in rocks, soils, and sediments, and the geochemistry of Mn means that these oxides can precipitate in a wide variety of geological settings. Their typical occurrence as fine-grained mixtures and/or poorly crystalline phases means that it is difficult to determine the mineralogy of Mn-oxides using X-ray powder diffraction (XRD) analysis alone. Here, we use both XRD and electron microprobe analyses to characterize individual Mn-oxides within the studied ore deposits.

The main Mn minerals that constitute the ores from San Pietro Island are pyrolusite, cryptomelane, and hollandite, with quartz, feldspar, and biotite as accessory phases. Coronadite and barite were detected only by SEM–EDS observation in samples from Cala Fico, whereas Opal-CT was observed both in outcrop and in thin section; however, the association between Opal-CT and Mn minerals precludes the possibility of establishing a precipitation sequence based on textural features. Micromorphological observations reveal that, in all hydrothermal samples, Mn minerals form a muddy matrix containing the accessory phases. K-feldspar is often intergrown with, or replaced by, Mn-oxides or Fe-bearing minerals. The accessory minerals determined by EDS microanalysis include sub-euhedral zircon, biotite (often replaced by pseudomorphic cryptomelane), apatite, monazite, and cerianite. Ce-oxides form amorphous aggregates, ranging in size from a few microns to tens of microns across, and appear to have grown within the Mn-oxide matrix.

In the sedimentary ores, we identified several Mn-oxides, including cryptomelane, vernadite, hollandite, lithiophorite, hausmannite, coronadite, birnessite, and ramsdellite. Only cryptomelane was observed in all samples; vernadite and hollandite are present in most samples, whereas the other Mn-oxides were rarely present. These oxides are commonly found as a weathering product in soils (Koppi et al., 1996; Post, 1999).

Microscopic (OM and/or SEM) examinations indicate that Mn-oxides occur as microcrystalline botryoidal concretions that overgrew strongly weathered fragments of volcanic material, mainly glassy xenoliths, quartz, plagioclase, and K-feldspar. The XRD data also indicated the presence of 2:1 clay minerals, goethite, and hematite in a small number of samples.

5.2. Chemistry

Elemental concentrations and ratios within both Mn ores and hydrothermally altered wall-rocks (comendite) are given in Table 1; chondrite-normalized (denoted by the subscript '$_{ch}$') REE patterns are shown in Fig. 3, and all show negative Eu anomalies, a feature observed in most Mn deposits through time (Maynard, 2010).

In hydrothermal Mn ores, MnO concentrations range from 31.16 to 79.95 wt.%, and CF samples have higher ΣREE concentrations (from 1029 to 3309 ppm) and increased fractionation of light REEs (LREEs) and heavy REEs (HREEs), with $(La/Yb)_{ch}$ ratios of 15.7–47.1, and more negative Eu anomalies (Eu/Eu*, <0.1) than the LP ores. LP samples have ΣREE contents of 423–982 ppm, with negative Eu anomalies of 0.15 to 0.64 and $(La/Yb)_{ch}$ ratios of 4.1–9.8. The concentrations and distributions of REEs and the presence of negative Eu anomalies suggest that the mineralizing solutions were rock-buffered. Higher ΣREE

Table 1
Chemical data.

	PC1	PC2	PC3	PC4	PC5	PC6	PC7	LP1	LP2	LP3	LP4	LP5	LP6	LP7	CF1	CF2	CF3	CF4	CF5	CF6	CF7	CF8	Comendite (wall-rock)
SiO_2	7.2	11.3	6.6	20.6	19.1	20.1	22.1	32.3	27.2	23.3	21.2	25.1	24.8	30.6	42.8	42.0	43.2	3.1	1.9	6.5	21.5	29.9	74.1
Al_2O_3	4.4	6.1	4.1	5.1	5.2	7.4	5.4	7.7	5.5	5.9	4.3	5.2	5.5	5.9	6.6	6.7	7.1	1.7	1.4	1.4	3.4	4.6	12.1
Fe_2O_3	2.3	3.5	1.1	1.4	1.1	2.1	1.7	2.3	1.5	1.7	1.3	3.1	1.7	1.6	1.8	1.7	1.9	0.1	0.0	0.2	1.5	2.6	3.2
MnO	51.1	49.9	60.1	45.2	48.8	43.3	47.4	40.2	47.3	53.7	58.9	52.2	48.8	44.5	31.3	35.4	29.9	70.5	80.0	72.9	53.1	49.1	0.1
MgO	0.4	0.7	0.3	0.3	0.1	0.3	0.1	0.4	0.5	0.4	0.1	0.2	0.6	0.2	0.2	0.1	0.1	0.2	0.1	0.6	0.1	0.1	0.1
CaO	0.3	0.5	0.4	0.4	0.4	0.6	0.5	0.8	0.7	0.8	0.2	0.4	0.9	0.7	0.2	0.1	0.1	0.2	0.1	0.4	0.1	0.2	0.1
Na_2O	0.4	0.4	0.4	0.8	0.9	0.8	1.4	2.4	0.9	1.6	1.2	0.4	1.1	1.7	1.8	2.6	2.4	0.5	0.4	0.0	1.1	1.9	4.6
K_2O	3.8	2.9	3.8	3.3	4.7	2.9	3.6	4.5	4.1	3.3	4.1	4.6	2.8	4.6	4.9	4.7	4.7	4.8	3.9	2.0	3.6	4.6	4.5
TiO_2	0.11	0.12	0.13	0.11	0.13	0.15	0.19	0.30	0.26	0.38	0.11	0.18	0.32	0.33	0.11	0.09	0.11	0.02	0.02	0.03	0.06	0.11	0.17
P_2O_5	0.87	0.56	0.92	0.51	0.50	0.17	0.28	0.51	0.17	0.21	0.28	0.29	0.17	0.37	0.01	0.03	0.05	0.02	0.02	0.02	0.01	0.02	0.01
LOI	13.8	14.7	13.0	10.3	10.2	11.5	9.0	7.2	10.1	9.6	9.1	8.0	10.9	7.0	10.3	6.2	6.3	11.7	11.7	16.0	9.1	6.8	1.0
Total	84.7	90.7	90.8	88.0	91.1	89.3	91.7	98.6	98.3	100.9	100.8	99.8	97.6	97.5	99.9	99.7	95.8	93.0	99.5	100.0	93.6	99.7	99.98
La	63.3	71.3	69.2	95.4	58.0	140.0	90.2	77.6	75.5	124.0	127.0	182.0	84.5	48.6	479.0	516.0	464.0	797.0	744.0	695.0	502.0	281.0	97.9
Ce	148	263	234	489	167	769	651	305	207	629	328	233	539	100	620	503	977	1420	563	634	1370	289	196
Pr	15.6	16.4	18.6	19.7	15.3	34.8	21.1	15.8	15.9	20.8	25.0	31.8	17.5	9.95	97.6	96.7	98.0	187.0	187.0	197.0	116.0	52.0	24.1
Nd	59.6	58.4	74.6	73.0	59.2	128.0	82.2	54.4	58.3	74.0	87.6	116.0	62.6	36.6	345.0	349.0	336.0	594.0	612.0	687.0	397.0	193.0	88.9
Sm	13.7	13.2	18.7	16.1	14.2	29.7	19.2	11.4	13.7	17.6	20.7	24.3	14.3	7.9	79.7	81.9	76.6	122.0	128.0	145.0	87.3	45.6	19.5
Eu	2.38	2.29	3.37	1.34	2.20	2.61	1.05	1.53	2.78	2.97	1.00	1.20	2.21	1.63	0.50	0.60	0.51	0.67	0.70	1.20	0.35	0.40	0.10
Gd	13.7	12.9	21.4	17.5	15.3	32.7	21.2	9.1	12.7	20.9	19.7	22.8	13.6	7.0	83.6	105.0	74.6	89.2	102.0	83.7	63.3	68.4	16.9
Tb	2.4	2.3	3.8	3.1	2.8	6.0	3.9	1.9	2.6	4.9	4.5	4.7	2.7	1.4	11.8	14.6	10.8	11.0	11.4	11.6	7.6	9.7	2.9
Dy	15.0	14.0	23.5	19.4	17.4	37.1	24.0	10.9	14.5	31.2	26.7	26.9	15.4	8.6	53.1	67.7	51.0	47.4	51.6	54.7	30.4	47.0	18.9
Ho	3.1	2.7	4.8	4.0	3.5	7.6	5.1	2.2	3.0	7.3	5.6	5.3	3.1	1.8	8.6	11.1	8.6	7.3	8.0	8.9	4.7	8.3	3.9
Er	8.9	8	14.5	11.9	10.2	22.8	15.4	6.4	8.4	22	15.9	14.7	8.7	5.3	20.2	25.8	20.8	17.7	19.4	21.5	11	19.2	11.2
Tm	1.3	1.2	2.2	1.8	1.5	3.51	2.37	1.04	1.1	3.29	2.22	2.1	1.26	0.74	2.7	3.3	2.8	2.39	2.6	2.7	1.4	2.5	1.8
Yb	8.4	8.0	14.9	12.2	9.7	23.1	16.3	6.3	6.5	20.3	13.4	12.5	8.2	4.7	14.1	15.7	14.6	12.1	12.9	13.9	7.2	12.1	10.7
Lu	1.32	1.27	2.38	1.98	1.55	3.72	2.69	0.90	1.00	3.32	2.09	1.90	1.28	0.72	1.80	2.00	1.85	1.39	1.50	1.70	0.90	1.60	1.54
ΣREE	356.70	474.96	505.95	766.42	377.85	1240.64	956.16	504.47	422.98	981.58	679.41	755.6	774.35	234.94	1885.5	1845.2	2137.16	3309.15	2514.8	2627.2	2599.15	1097.3	494.34
Eu/Eu*	0.53	0.54	0.51	0.24	0.46	0.26	0.23	0.46	0.64	0.47	0.15	0.16	0.48	0.67	0.02	0.02	0.02	0.02	0.02	0.03	0.01	0.02	0.02
Ce/Ce*	1.08	1.75	1.51	2.53	1.29	2.53	3.40	1.95	1.34	2.68	1.30	0.67	3.15	1.02	0.64	0.50	1.03	0.84	0.35	0.40	1.29	0.53	0.93
$(La/Yb)_{ch}$	5.09	6.02	3.14	5.28	4.04	4.10	3.74	8.32	7.85	4.13	6.40	9.84	6.96	6.99	22.96	22.21	21.48	44.51	33.97	33.79	47.11	15.69	6.20

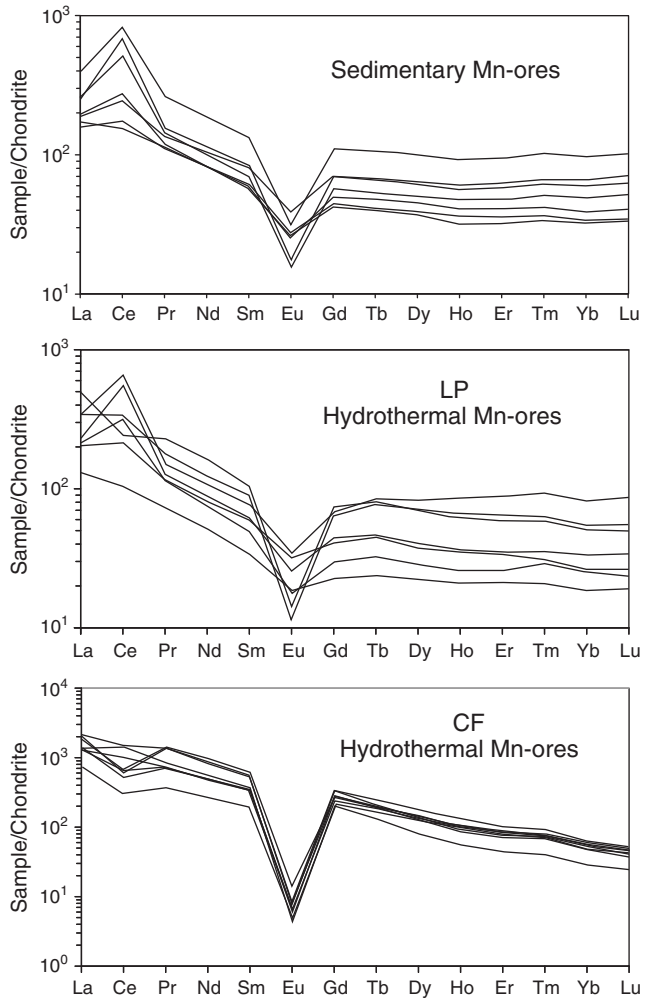

Fig. 3. Chondrite-normalized REE patterns.

concentrations, higher $(La/Yb)_{ch}$ ratios, and strongly negative Eu anomalies reflect interaction with the highly evolved comenditic lava, whereas moderately negative Eu anomalies and flatter REE patterns suggest interaction with the less evolved rhyolitic ignimbrite (Sinisi et al., 2012). Furthermore, Ce anomalies in the LP samples are generally positive (1.02–3.15, with the exception of sample LP5, which has a Ce/Ce* ratio of 0.67), whereas only one sample from the CF area has a positive Ce anomaly (CF7, with a Ce/Ce* ratio of 1.29); CF3 has a negligible Ce anomaly (CF3 with a Ce/Ce* ratio of 1.03), and the remaining CF samples have negative Ce anomalies, ranging between 0.35 and 0.84.

In the sedimentary Mn ores, MnO concentrations vary between 43.30 and 60.09 wt.%. In PC samples, ΣREE concentrations are 356–1240 ppm with Eu anomalies of 0.23–0.54. The magnitude of the negative Eu anomaly roughly correlates with increasing Al_2O_3 concentrations, suggesting that feldspar hosts the majority of the Eu within the ores. Fractionation of REEs is moderate, with $(La/Yb)_{ch}$ ratios of 3.14–6.02, and all samples have positive Ce anomalies, with Ce/Ce* ratios of 1.08–3.40, as commonly observed in Mn-oxide-rich soils formed during pedogenesis (Laveuf et al., 2012, and references therein). In these ores organic matter has not been detected.

6. Discussion

6.1. Ce anomalies in sedimentary Mn ores

The sorption of REEs onto Mn-oxides is one of the main mechanisms of REE scavenging in soils, because under typical pH conditions, the zero charge nature of Mn-oxides makes them capable of having a negative residual charge. This, in turn, generates a higher capacity and a higher rate of REE sorption than that of Fe-oxides under the same conditions (Laveuf and Cornu, 2009, and references therein).

In natural soil, the importance of Mn-oxides in trapping Ce and therefore generating positive Ce anomalies is well documented, and has been used to identify redox processes during pedogenesis (Feng, 2010; Laveuf and Cornu, 2009; Laveuf et al., 2012; Palumbo et al., 2001; Rankin and Childs, 1976). Positive Ce anomalies are linked to the oxidation of Ce(III) to Ce(IV), leading to the precipitation of cerianite, coupled with the reduction of Mn(IV) on the surface of Mn-oxides. This oxidative scavenging is a three-stage process (Bau, 1999), comprising (1) initial sorption of trivalent REE onto Mn oxyhydroxides, followed by (2) oxidation of Ce by surface catalysis on Mn hydroxides (Koeppenkastrop and De Carlo, 1992; Koppi et al., 1996; Ohta and Kawabe, 2001; Takahashi et al., 2000), and (3) the preferential desorption of trivalent REEs, including Ce(III) preferential to Ce(IV).

Assuming that many redox cycles occur during soil formation and development, Laveuf et al. (2012) stated that during the reduction phase of these redox cycles, Mn-oxides partially dissolve, whereas cerianite, the stability of which is controlled by changes in pH rather than Eh, does not. During subsequent oxidation, Mn-oxides precipitate and incorporate more Ce, probably as cerianite. Such a Mn-oxide dissolution/precipitation process leads to a progressive enrichment of cerianite in Mn concretions and increases the magnitude of the positive Ce anomaly of the soil. This suggests that the magnitude of the positive Ce anomaly, as a proxy for the abundance of cerianite, could trace changes in redox conditions during the Mn-oxide precipitation/dissolution cycle.

It should be noted that differences in the REE characteristics of pedogenetic Mn-oxides have been related to a preferential association between REEs and other soil components, such as organic matter (e.g., Davranche et al., 2005, 2008; Pourret et al., 2010). Furthermore, Dia et al. (2000) and Seto and Akagi (2008) suggested that Ce cannot be used as a tracer of redox conditions in organic-rich environments. Pourret et al. (2010) used spatial variations in Ce anomalies to indicate the presence of two distinct sources of REEs in shallow groundwaters: (2) REEs that were soluble under organic-free, oxidizing conditions, characterized by a large negative Ce anomaly; and (2) REEs that were dissolved in an organic-rich environment, with no negative Ce anomaly. The presence of organic matter inhibits the development of negative Ce anomalies in oxidizing waters because Ce cannot be oxidized at the surface of Mn oxides, and, more importantly, because all of the REEs form complexes with organic molecules, meaning that Ce is not selectively removed from the solution (Davranche et al., 2005, 2008).

In our study, the large range in positive Ce anomalies, from 1.08 to 3.40, may relate to variation between organic-rich and organic-poor environments during the period of formation of Mn ores. Samples with very low positive Ce anomalies (Ce/Ce* of 1.08; sample PC1) to low positive Ce anomalies (Ce/Ce* from 1.25 to 1.75; samples PC2, PC3, and PC5) most likely formed in an environment where organic speciation and the formation of organic-REE complexes had a marked limiting effect on cerianite precipitation, and therefore attenuated the development of positive Ce anomalies. The fact that Ce anomaly-free organic colloids are concentrated in organic-rich soil horizons (Pourret et al., 2010) links well with the fact that all samples with weakly positive Ce/Ce* ratios (1.08–1.75) are either from thick beds within paleosoils (samples PC1, PC2, PC3, and PC5) or from veins originating within paleosoil (sample PC4). Conversely, samples with large positive Ce anomalies (Ce/Ce* > 2.5; samples PC4, PC6, and PC7) are spheroidal concretions of Mn-oxides within pumice and ash, and likely formed in an environment with little or no organic matter, where REE speciation in circulating fluids was dominated by inorganic species.

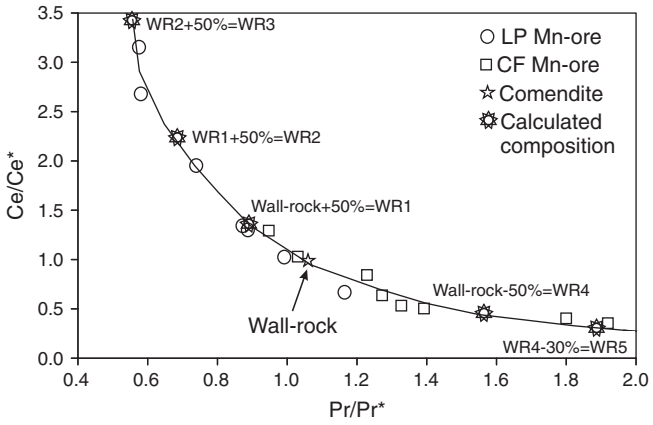

Fig. 4. Ce/Ce* vs. Pr/Pr* plot. See text for further details.

6.2. Ce-anomalies in hydrothermal Mn ores

The mobility of REEs in hydrothermal systems is controlled by the availability of complexing ions such as CO_3^{2-}, PO_4^{3-}, F^-, SO_4^{2-}, and Cl^-, and is promoted by low pH and a high water/rock ratio (Haas et al., 1995). However, in addition to the fluid composition, the concentration of REEs in hydrothermal fluids is controlled by temperature, pressure, crystallo-chemical factors, and reaction kinetics, making it difficult to determine the origin and fate of REE-bearing fluids in ancient hydrothermal systems (Gieré, 1996).

The formation of the Sardinian hydrothermal Mn ores involved the mixing of a magmatic fluid with meteoric water in the shallow crust (Sinisi et al., 2012). Vein fills are generally brecciated and include wall-rock fragments with clinoptilolite occurring along wall-rock selvages. The presence of clinoptilolite indicates that mineralizing fluids were slightly alkaline (Zhang et al., 2001), probably due to interaction with alkaline or peralkaline rocks, such as rhyolites and comendites; these alkaline conditions did not favor large-scale REE mobility.

One attribute of the hydrothermal Mn ores worth further discussion is the fluctuation of Ce anomaly values. Chetty and Gutzmer (2011), in a study of the hydrothermal alteration of Mn ores,, interpreted these fluctuations to reflect local remobilization of REEs during hydrothermal dissolution of apatite, the redistribution of other accessory minerals including cerianite, and the dissolution and reprecipitation of REE-bearing minerals. In the Ce/Ce* vs. Pr/Pr* plot (Bau and Dulski, 1996) they modeled the depletion and the enrichment of Ce, starting from the average composition of the unaltered rock, demonstrating that altered rocks fall on a power curve. The calculated concentrations were obtained making new host compositions out of derived compositions and adding or subtracting Ce from these new host compositions. The measured data greatly fitted the modeled curve.

Here, we modeled a power law curve by adding and subtracting Ce from a starting point defined by the composition of a comendite sample from San Pietro Island; the measured compositions of all hydrothermal Mn ores fall close to or on the modeled curve (Fig. 4). According to Chetty and Gutzmer's (2011) modeling of the dissolution and redistribution of REE accessory minerals, this involves: (1) removal of REEs from wall-rocks by hydrothermal fluids; (2) precipitation of newly formed REE-bearing minerals, including cerianite, within the Mn-ores from the hydrothermal fluids, resulting in positive Ce anomalies; and (3) precipitation of REE-bearing minerals from the Ce-depleted hydrothermal fluid, giving rise to negative Ce anomalies. This is consistent

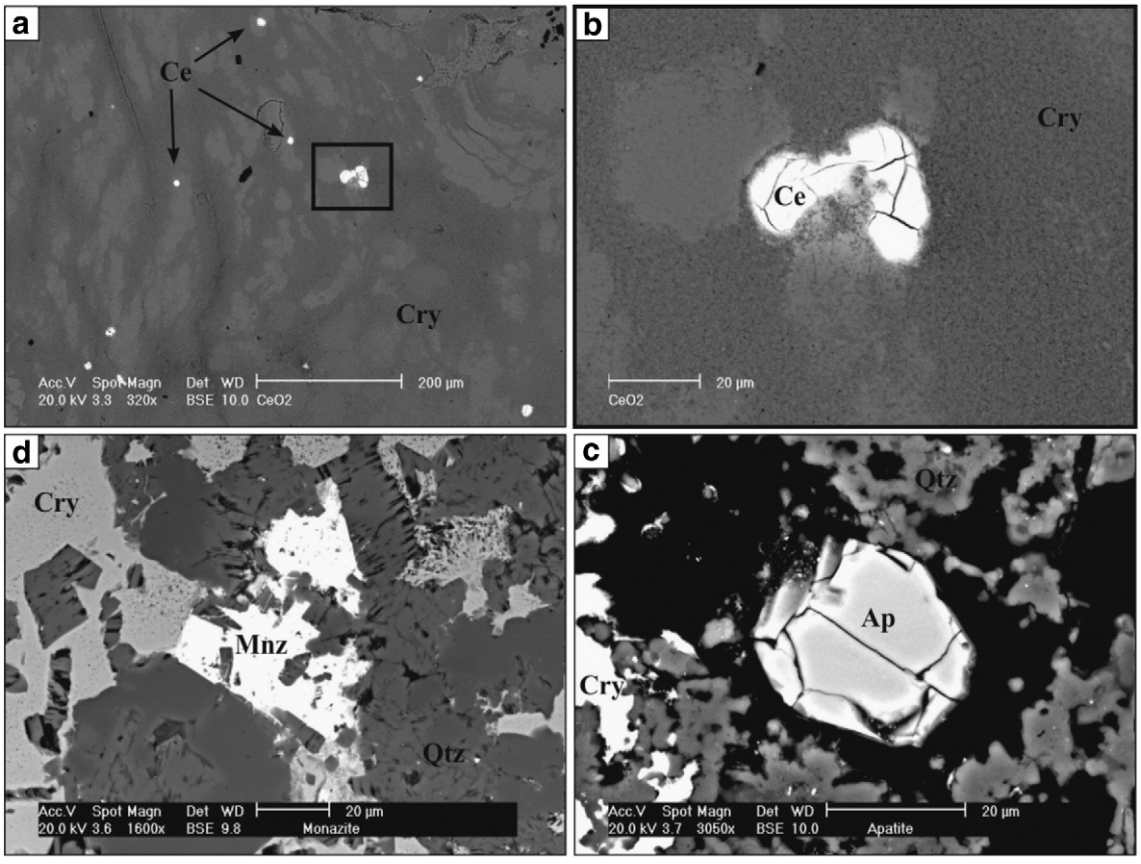

Fig. 5. SEM microphotographs showing REE-bearing minerals in hydrothermal samples. Ce = cerianite; Mnz = monazite; Ap = apatite; Cry = cryptomelane; Qtz = quartz.

with the occurrence of apatite, monazite, and cerianite, which grew within the Mn-oxide matrix of the hydrothermal ores (Fig. 5).

It is also worth noting that at La Piramide, this redistribution increases the magnitude of the positive Ce anomaly, whereas Ce depletion is observed at the Cala Fico site. This result suggests that the mineralizing fluid moved from LP to CF along the E–W-striking fault proximal to the Mn-ores.

7. Summary

The Mn ores of south-western Sardinia are both sedimentary and hydrothermal in origin, contain high concentrations of REEs, and are characterized by large Ce/Ce* fluctuations, especially in the hydrothermal ores. The origin of the Ce/Ce* fluctuations in the hydrothermal Mn ores is related to remobilization of REEs within the hydrothermal system, involving the dissolution and redistribution of REE accessory minerals from wall-rocks to Mn-ores by the mineralizing fluid.

This model is consistent with (1) the fact that the observed data fit a modeled Ce/Ce* vs. Pr/Pr* curve, starting from the average wall-rock composition, and adding or subtracting Ce; and (2) the occurrence of secondary REE minerals (e.g., apatite, monazite, and cerianite) in the Mn-oxide matrix within the ores.

The variability of Ce anomalies in the sedimentary pedogenic Mn ores most likely relates to differences between organic-rich and organic-poor environments. Low to very low positive Ce anomalies (1.08–1.75) are found in samples from thick beds within paleosoils or from paleosoil-related veins, and possibly formed in an environment where organic speciation of REEs acted to limit cerianite precipitation. This is consistent with the fact that Ce-anomaly-free organic colloids are concentrated in organic-rich soil horizons. Conversely, samples having larger positive Ce anomalies ($Ce/Ce^* > 2.5$) consist of spheroidal concretions of Mn-oxides within pumice and ash, and likely formed in organic-free, or low-organic, environments, with speciation of REEs in circulating fluids dominated by inorganic species.

Finally, given that large Ce/Ce* fluctuations are associated with Mn ores, in order to avoid erroneous interpretations of Ce anomalies, we highlight the recommendations of Chetty and Gutzmer (2011) relating to the sampling of hydrothermal Mn-ores, and extend these recommendations to associated sedimentary Mn deposits, if present. The use of these recommended methodologies should avoid reaching erroneous conclusions relating to the mechanisms of Ce distribution and the relationships between Ce and Mn phases.

Acknowledgments

We are grateful to A. Laurita, CIGAS, University of Basilicata, for ESEM–EDS facilities. Financial support was provided by the 'Banco di Sardegna' Foundation. Comments from two anonymous reviewers improved the manuscript.

References

Assorgia, A., Fadda, A., Torrente, D.G., Morra, V., Ottelli, L., Secchi, F.A., 1990. Le successioni ignimbritiche terziare del Sulcis (Sardegna sud-occidentale). Memorie della Societa Geologica Italiana 45, 951–963.

Bau, M., 1991. Rare earth element mobility during hydrothermal and metamorphic fluid–rock interaction and the significance of the oxidation state of europium. Chemical Geology 93, 219–230.

Bau, M., Dulski, P., 1996. Distribution of yttrium and rare-earth elements in the Penge and Kuruman iron-formations, Transvaal Supergroup, South Africa. Precambrian Research 79, 37–55.

Bau, M., 1999. Scavenging of dissolved yttrium and rare earths by precipitating iron oxyhydroxide: experimental evidence for Ce oxidation, Y–Ho fractionation, and lanthanide tetrad effect. Geochimica et Cosmochimica Acta 63, 67–77.

Beccaluva, L., Brotzu, P., Macciotta, G., Morbidelli, L., Serri, G., Traversa, G., 1987. Caenozoic tectono-magmatic evolution and inferred mantle sources in the Sardo-Tyrrhenian area. In: Boriani, A., Bonafede, M., Piccardo, G.B., Vai, G.B. (Eds.), The Lithosphere in Italy — Advances in Earth Science Research. Accademia Nazionale dei Lincei, pp. 229–248.

Braun, J.J., Pagel, M., Muller, J.P., Bilong, P., Michard, A., Guillet, B., 1990. Cerium anomalies in lateritic profiles. Geochimica et Cosmochimica Acta 54, 781–795.

Braun, J.J., Viers, J., Dupré, B., Polve, M., Ndam, J., Muller, J.P., 1998. Solid/liquid REE fractionation in the lateritic system of Goyoum, East Cameroon: the implication for the present dynamics of the soil covers of the humid tropical regions. Geochimica et Cosmochimica Acta 62, 273–299.

Chang-Bock, I., Sang-Mo, K., Ho-Wan, Ch., Tetsuichi, T., 2002. The geochemical behaviour of altered igneous rocks in the Tertiary Gampo Basin, Kyongsang. Geochemical Journal 36, 391–407.

Chetty, D., Gutzmer, J., 2011. REE redistribution during hydrothermal alteration of ores of the Kalahari manganese deposit. Ore Geology Reviews http://dx.doi.org/10.1016/j.oregeorev.2011.06.001.

Class, C., le Roex, A.P., 2008. Ce anomalies in Gough Island lavas — trace element characteristics of a recycled sediment component. Earth and Planetary Science Letters 265, 475–486.

Coulon, C., Dostal, J., Dupy, C., 1978. Petrology and geochemistry of the ignimbrites and associated lava domes of N.W. Sardinia. Contributions to Mineralogy and Petrology 68, 89–98.

Davranche, M., Pourret, O., Gruau, G., Dia, A., Le Coz-Bouhnik, M., 2005. Adsorption of REE(III)-humate complexes onto MnO_2: experimental evidence for cerium anomaly and lanthanide tetrad effect suppression. Geochimica et Cosmochimica Acta 69, 4825–4835.

Davranche, M., Pourret, O., Gruau, G., Dia, A., Jin, D., Gaertner, D., 2008. Competitive binding of REE to humic acid and manganese oxide: impact of reaction kinetics on development of Cerium anomaly and REE adsorption. Chemical Geology 247, 154–170.

De Baar, H.J.W., Bacon, M.P., Brewer, P.G., 1983. Rare earth distributions with a positive Ce anomaly in the western North Atlantic Ocean. Nature 301, 324–327.

de Boorder, H., Spakman, W., White, S.H., Wortel, M.J.R., 1998. Late Cenozoic mineralization, orogenic collapse and s detachment in the European Alpine Belt. Earth and Planetary Science Letters 164, 569–575.

De Carlo, E.H., Wen, X.-Y., Irving, M., 1998. The influence of redox reactions on the uptake of dissolved Ce by suspended Fe and Mn oxide particles. Aquatic Geochemistry 3, 357–389.

Dia, A., Gruau, G., Olivié-Lauquet, G., Riou, C., Molenat, J., Curmi, P., 2000. The distribution of rare earth elements in groundwaters: assessing the role of source-rock composition, redox changes and colloidal particles. Geochimica et Cosmochimica Acta 64, 4131–4151.

Downes, H., Thirlwall, M.F., Trayhorn, S.C., 2001. Miocene subduction-related magmatism in southern Sardinia: Sr–Nd- and oxygen isotopic evidence for mantle source enrichment. Journal of Volcanology and Geothermal Research 106, 1–22.

Feng, J., 2010. Behaviour of rare earth elements and yttrium in ferromanganese concretions, gibbsite spots, and the surrounding terra rossa over dolomite during chemical weathering. Chemical Geology 271, 112–132.

Fulignati, P., Gioncada, A., Sbrana, A., 1999. Rare earth element (REE) behaviour in alteration facies of the active magmatic–hydrothermal system of Volcano (Aeolin Island, Italy). Journal of Volcanology and Geothermal Research 88, 325–342.

Gieré, R., 1996. Formation of rare earth minerals in hydrothermal systems. In: Jones, A.P., Wall, F., Williams, C.T. (Eds.), Rare Earth Minerals. Chemistry, Origin and Ore Deposits. : The Mineralogical Society Series 7. Chapman & Hall, London. 372 pp.

Haas, J.R., Shock, E.L., Sassani, D.C., 1995. Rare earth elements in hydrothermal systems: estimates of standard partial molar thermodynamic properties of aqueous complexes of the rare earth elements at high pressures and temperatures. Geochimica et Cosmochimica Acta 59, 4329–4350.

Kerrich, R., Said, N., 2011. Extreme positive Ce-anomalies in a 3.0 Ga submarine volcanic sequence, Murchison Province: oxygenated marine bottom waters. Chemical Geology 280, 232–241.

Koeppenkastrop, D., De Carlo, E.H., 1992. Sorption of rare-earth elements from seawater onto synthetic mineral particles: an experimental approach. Chemical Geology 95, 251–263.

Koppi, A.J., Edis, R., Field, D.J., Geering, H.R., Klessa, D.A., Cockayne, D.J., 1996. Rare earth elements trend and cerium–uranium–manganese association in weathered rock from Koongarra, Northern Territory, Australia. Geochimica et Cosmochimica Acta 60, 1695–1707.

Laveuf, C., Cornu, S., 2009. A review on the potentiality of rare earth elements to trace pedogenetic processes. Geoderma 154, 1–12.

Laveuf, C., Cornu, S., Guilherme, L.R.G., Guerin, A., Juillot, F., 2012. The impact of redox conditions on the rare earth element signature of redoximorphic features in a soil sequence developed from limestone. Geoderma 170, 25–38.

Leybourne, M.I., Johannesson, K.H., 2008. Rare earth elements (REE) and yttrium in stream waters, stream sediments, and Fe–Mn oxyhydroxides: fractionation, speciation, and controls over REE + Y patterns in the surface environment. Geochimica et Cosmochimica Acta 72, 5962–5983.

Lottermoser, B.G., 1992. Rare earth element and hydrothermal ore formation processes. Ore Geology Reviews 7, 25–41.

Lustrino, M., Morra, V., Fedele, L., Franciosi, L., 2009. Beginning of the Apennine subduction system in central western Mediterranean: constraints from Cenozoic "orogenic" magmatic activity of Sardinia, Italy. Tectonics 28, TC5016 http://dx.doi.org/10.1029/2008TC002419.

Maynard, J.B., 2010. The chemistry of manganese ores through time: a signal of increasing diversity of earth-surface environments. Economic Geology 105, 535–552.

Moffett, J.W., 1990. Microbially mediated cerium oxidation in sea water. Nature 345, 421–423.

Moffett, J.W., 1994. A radiotracer study of cerium and manganese uptake onto suspended particle in Chesapeake Bay. Geochimica et Cosmochimica Acta 58, 695–703.
Mongelli, G., 1997. Ce-anomalies in the textural components of Upper Cretaceous karst bauxites from the Apulian carbonate platform (southern Italy). Chemical Geology 140, 69–79.
Morra, V., Secchi, F., Assorgia, A., 1994. Petrogenetic significance of peralkaline rocks from Cenozoic calc-alkaline volcanism from SW Sardinia, Italy. Chemical Geology 118, 109–142.
Ohnuki, T., Ozaki, T., Kozai, N., Nankawa, T., Sakamoto, F., Sakai, T., Suzuki, Y., Francis, A.J., 2008. Concurrent transformation of Ce(III) and formation of biogenic manganese oxides. Chemical Geology 253, 23–29.
Ohta, A., Kawabe, I., 2001. REE(III) adsorption onto Mn dioxide (δ-MnO_2) and Fe oxyhydroxide: Ce(III) oxidation by δ-MnO_2. Geochimica et Cosmochimica Acta 65, 695–703.
Palumbo, B., Bellanca, A., Neri, R., Roe, M.J., 2001. Trace metal partitioning in Fe–Mn nodules from Sicilian soils, Italy. Chemical Geology 173, 257–269.
Parsapoor, A., Khalili, M., Mackizadeh, M.A., 2009. The behaviour of trace and rare earth elements (REE) during hydrothermal alteration in the Rangan area (Central Iran). Journal of Asian Earth Sciences 34, 123–134.
Pioli, L., Rosi, M., 2005. Rheomorphic structures in a high-grade ignimbrite: the Nuraxi tuff, Sulcis volcanic district (SW Sardinia, Italy). Journal of Volcanology and Geothermal Research 142, 11–28.
Post, J.E., 1999. Manganese oxide minerals: crystal structures and economic and environmental significance. Proceedings of the National Academy of Sciences of the United States of America 96, 3447–3454.
Pourret, O., Gruau, G., Dia, A., Davranche, M., Molenat, J., 2010. Colloidal control on the distribution of rare earth elements in shallow groundwaters. Aquatic Geochemistry 16, 31–59.
Rankin, P.C., Childs, C.W., 1976. Rare-earth elements in iron–manganese concretions from some New Zealand soils. Chemical Geology 18, 55–64.
Seto, M., Akagi, T., 2008. Chemical condition for the appearance of a negative Ce anomaly in stream waters and groundwaters. Geochemical Journal 42, 371–380.
Sinisi, R., Mameli, P., Mongelli, G., Oggiano, G., 2012. Different Mn-ores in a continental arc setting: geochemical and mineralogical evidences from Tertiary deposits of Sardinia (Italy). Ore Geology Reviews 47, 110–125.
Smith, P., Henderson, P., Campbell, L.S., 2000. Fractionation of the REE during hydrothermal processes: constraints from the Bayan Obo Fe–REE–Nb deposit, Inner Mongolia, China. Geochimica et Cosmochimica Acta 64 (18), 3141–3160.
Takahashi, Y., Shimizu, H., Usui, A., Kagi, H., Nomura, M., 2000. Direct observation of tetravalent cerium in ferromanganese nodules and crusts by X-ray-absorption near edge structure (XANES). Geochimica et Cosmochimica Acta 64, 2929–2935.
Tanaka, K., Tani, Y., Takahashi, Y., Tanimizu, M., Suzuki, Y., Kozai, N., Ohnuki, T., 2010. A specific Ce oxidation process during sorption of rare earth elements on biogenic Mn oxide produced by *Acremonium* sp. strain KR21-2. Geochimica et Cosmochimica Acta 74, 5463–5477.
Terakado, Y., Fujitani, T., 1998. Behaviour of the rare earth elements and other trace elements during interactions between acidic hydrothermal solutions and silicic volcanic rocks, southwestern Japan. Geochimica et Cosmochimica Acta 62, 1903–1917.
Zhang, S., Zhao, P., Xu, Z., Zheng, M., 2001. Water/rock interactions and changes in chemical composition during zeolite mineralization. Chinese Journal of Geochemistry 20, 226–232.